

# PCCP

Accepted Manuscript



This is an *Accepted Manuscript*, which has been through the Royal Society of Chemistry peer review process and has been accepted for publication.

*Accepted Manuscripts* are published online shortly after acceptance, before technical editing, formatting and proof reading. Using this free service, authors can make their results available to the community, in citable form, before we publish the edited article. We will replace this *Accepted Manuscript* with the edited and formatted *Advance Article* as soon as it is available.

You can find more information about *Accepted Manuscripts* in the [Information for Authors](#).

Please note that technical editing may introduce minor changes to the text and/or graphics, which may alter content. The journal's standard [Terms & Conditions](#) and the [Ethical guidelines](#) still apply. In no event shall the Royal Society of Chemistry be held responsible for any errors or omissions in this *Accepted Manuscript* or any consequences arising from the use of any information it contains.

**Unusual Denaturation Trajectory of Bovine Gamma Globulin****Studied by Fluorescence Correlation Spectroscopy**

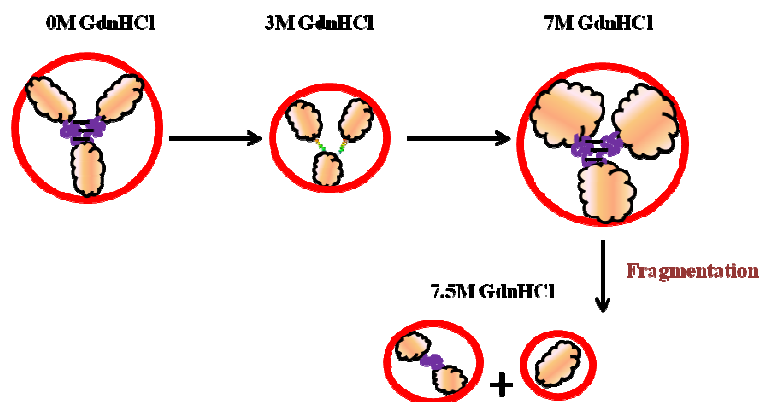
Moupriya Nag<sup>†</sup>, Debajyoti Das<sup>‡</sup>, Diptankar Bandyopadhyay<sup>§</sup>, Soumen Basak<sup>†\*</sup>

<sup>†</sup>Chemical Sciences Division, Saha Institute of Nuclear Physics, <sup>‡</sup>Department of Biophysics, Molecular Biology and Bioinformatics, <sup>§</sup>Department of Biochemistry, University of Calcutta

\*Corresponding author: Fax: (91)-33-2337 4637.

E-mail address: soumen.basak@saha.ac.in, soumenbasak08@gmail.com

## Table of Content



**Abstract:**

Non-native and denatured states of proteins have received increasing attention because of their relevance to issues such as protein folding and stability. In this context, the pathway of polypeptide collapse and random coil formation in a denatured protein is a subject of much interest. Most proteins so far studied have shown monotonic expansion of their hydrodynamic radius ( $R_H$ ) in presence of increasing concentration of chaotropes. We have studied GdnHCl-induced folding transitions and conformational states of a multi-domain protein, bovine gamma globulin, using fluorescence, circular dichroism and fluorescence correlation spectroscopy (FCS). FCS measurements showed that for gamma globulin, contrary to the observed trend,  $R_H$  decreases with increasing GdnHCl concentration up to 3 M. At higher GdnHCl concentration,  $R_H$  starts to increase but exhibits complicated behavior in the form of two sharp maxima at 4 M and 7 M. Further experiments suggest that the maximum at 4 M GdnHCl arises due to electrostatic interaction, whereas the one at 7 M GdnHCl corresponds to the usual expanded conformation due to denaturation. Beyond 7 M GdnHCl,  $R_H$  decreases drastically and is shown to result from fragmentation of the protein caused by rupture of disulphide bonds by the high GdnHCl concentration. Our results demonstrate the capability of FCS in revealing intricate details of the unfolding trajectory that elude conventional ensemble techniques such as fluorescence and CD.

## Introduction

In the ongoing quest for understanding the mechanism and pathway of protein denaturation, a detailed description of the partially or fully denatured state of proteins remains an important unresolved issue. An increasing number of studies are thus focusing on the conformation and dynamics of proteins in their extended state using ensemble or single molecular techniques [1,2]. Protein denaturation is a highly heterogeneous process in which rarely populated intermediate states may play an important role. Single-molecule techniques are ideally suited to resolve these heterogeneities [3-5]. Most unfolding studies focus on polypeptide chains of single domain proteins. Although the same basic principles should also apply to the folding of individual domains of multi-domain proteins, interaction between domains is expected to play a central role in their stability, dynamics of unfolding and aggregation [6,7].

Gamma globulins ( $\gamma$ G) are globular serum proteins of which the most significant fractions are immunoglobulins, also known as antibodies [8]. Antibodies are Y-shaped molecules that have two different functions: they bind antigens such as bacteria and viruses and induce a series of other 'effector functions' as a result of antigen binding. Their generic Y-shaped structure consists of four polypeptide chains: two pairs of identical light (MW 22-23 kD) and heavy (MW 50-70 kD) chains, with each light and heavy chain combination arranged as one arm of the Y ( $F_{ab}$  segment) [9-11]. The heavy chains, which extend to form the base of the Y ( $F_c$  segment), are interconnected through disulphide bonds, with several more disulphides being present in and between the light and heavy chains [12]. The spatial arrangement of these four polypeptide chains into separate compact globular regions, called fragments or domains, is key to its various biological functions such as antigen

recognition and binding. The disulphides are susceptible to chemical modification that, in turn, can generate structural variants and have a strong impact on the overall behavior of these proteins.

Rowe and Tanford (1973) have proposed the existence of partly denatured intermediates of immunoglobulin, though no stable intermediates have yet been identified. Goto et al. (1988) suggested that the denaturation of the immunoglobulin fragments,  $F_{ab}$  and  $F_c$ , is best described as a two-state process. Vermeer et al. have investigated the effect of temperature and role of hydrophobic interactions in understanding the stability of immunoglobulin using differential scanning calorimetry (DSC) and CD spectroscopy [13-18]. However, these studies failed to elucidate to what extent the denaturation of immunoglobulin is reversible, how it depends on the solution conditions, and whether the denaturation mechanism is cooperative.

In the present paper, we have studied GdnHCl-induced denaturation of bovine gamma globulin using fluorescence and circular dichroism spectroscopy and fluorescence correlation spectroscopy (FCS). With the potential to monitor events on time scales from nanoseconds to seconds, FCS has emerged as a sensitive tool for characterizing the dynamics of systems of biophysical and biochemical interest [19-21]. FCS correlates fluctuations in emission intensities arising from diffusion of fluorophores through a small confocal volume, rendering a convenient means to assess the characteristic diffusion time and hydrodynamic radius of the diffusing species. The overall results obtained by conventional fluorescence spectroscopy and FCS were consistent and indicated that denaturation of gamma globulin is reversible for GdnHCl concentrations up to 6 M. However, use of FCS revealed many more unexpected features of the unfolding trajectory

than shown by fluorescence and CD measurements. In addition, it was found that GdnHCl fragments the protein through disruption of the disulphide bonds.

## Results and Discussion

### Fluorescence spectroscopy

The emission maximum ( $\lambda_{\max}$ ) of tryptophan emission from native  $\gamma$ G occurs at  $\sim 340$  nm. Fig. 1 shows that upon denaturation in presence of increasing concentration of GdnHCl,  $\lambda_{\max}$  increases in sigmoidal fashion, signifying cooperative transition between the native and denatured states of  $\gamma$ G. Fitting the data in Fig. 1 to a sigmoidal function gave a value of  $(2.45 \pm 0.05)$  M for the midpoint of the transition ( $C_m$ ). Fig. 1 also shows the values of  $\lambda_{\max}$  obtained when  $\gamma$ G, after being treated by progressively increasing concentration of GdnHCl up to 6 M, was allowed to fold back from its denatured state by stepwise dilution of GdnHCl with buffer. The  $\lambda_{\max}$  vs. [GdnHCl] data obtained during the course of denaturation and renaturation superpose very closely, indicating that the trajectory of the unfolding transition was fully reversible from the denatured state in 6 M GdnHCl. However, renaturation from the denatured state at 7.5 M GdnHCl yielded a value of  $\lambda_{\max} = 357$  nm at 1 M GdnHCl, which is very different from its value (342 nm) obtained for the same concentration of GdnHCl during denaturation from the native state (Fig. 1). This result indicated that the protein lost its structural integrity to a major extent when subjected to such high GdnHCl concentration (7.5 M).

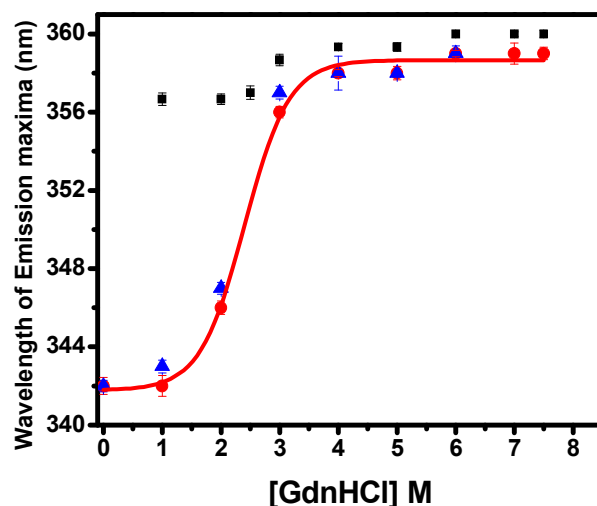


Fig. 1 Change in wavelength of Trp emission maxima of  $\gamma$ G in presence of varying concentration of GdnHCl during unfolding (●) from the native state and refolding from 6 M (▲) and 7.5 M (■) GdnHCl. The solid line represents a sigmoidal fit of the data for unfolding from the native state.

### Circular Dichroism spectroscopy

CD spectroscopy is widely used to monitor the loss of folded structure of a protein during denaturation [22]. In most cases, denaturation entails the loss of secondary structural motifs such as alpha helix or beta sheet and concomitant enhancement of random coil features. The CD spectra in Fig. 2a represent the changing secondary structural features of  $\gamma$ G on being presented with increasing GdnHCl concentration. The shape of the plot of the mean residue ellipticity at 218 nm ( $\theta_{218}$ ) vs. GdnHCl concentration (Fig. 2b) confirms the cooperative nature of the unfolding transition. Fitting the data in Fig. 2b to a sigmoidal function yields a value of  $(2.95 \pm 0.15)$  M for  $C_m$ , which is somewhat higher than its value ( $\sim 2.5$  M) obtained from fluorescence measurement (Fig. 1). This small difference may

signify a minor departure from a simple two-state unfolding of  $\gamma G$ , which is not unexpected for a large multi-domain protein [23].

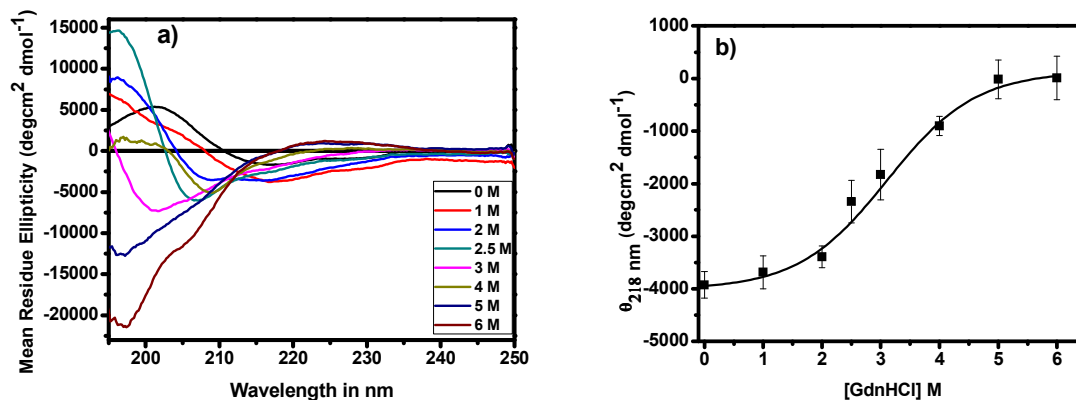


Fig. 2 a) Far-UV CD spectra of  $\gamma G$  in presence of varying concentrations of GdnHCl. b) Plot of mean residue ellipticity at 218 nm ( $\theta_{218}$ ) vs. GdnHCl concentration, superposed with a fit of the data points to a sigmoidal function.

A number of algorithms exist which use the far-UV CD spectra to provide an estimate of the secondary structure composition of proteins. We have employed the widely used algorithm CDSSTR [24-26] to calculate the relative proportions of various secondary structure elements in  $\gamma G$  at different GdnHCl concentrations (Table S1). The NRMSD values, which indicate the accuracy of fit of the calculated spectra with the experimental ones, were less than 0.03 in most cases, allowing us to conclude that the quality of the fits were good [27].

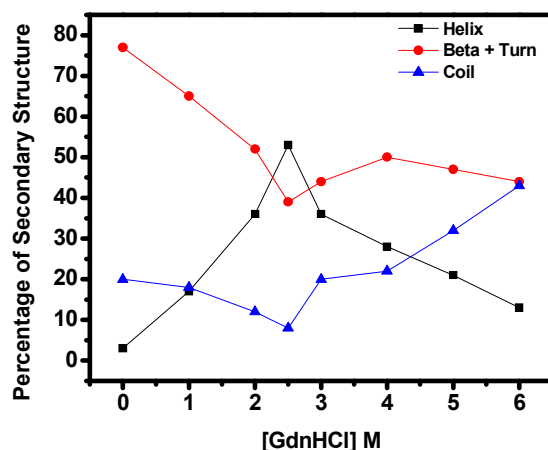


Fig. 3 Plot of secondary structure percentages (alpha, beta+turn, coil) as function of GdnHCl concentration emerging from fits of the CD spectra in Fig. 2(a).

Fig. 3 shows a plot of the percentages of secondary structure elements as function of GdnHCl concentration. It shows that with increase of GdnHCl concentration from 0 to 2.5 M, there is a steady increase in the helix content of  $\gamma$ G as well as decrease in the beta sheet, turn and random coil contents, suggesting that increasing GdnHCl concentrations up to 2.5 M actually induces a transition from random coil and sheet structure to  $\alpha$ -helical segments in  $\gamma$ G. Although prediction of exact region(s) in  $\gamma$ G where this transformation occurs is not possible, one may speculate that it involves the hinge region connecting the two arms of the Y to the base, where the solvent accessibility is higher than in other regions of the protein [12, 28].

### Fluorescence Correlation Spectroscopy (FCS)

To obtain information about how the conformational properties of  $\gamma$ G change during denaturation in more detail than that provided by the ensemble spectroscopic techniques of

fluorescence and CD spectroscopy, its diffusive behavior in solutions with varying GdnHCl concentration was explored with FCS. FCS allows determination of the mobility of fluorescent molecules in solution by fitting the autocorrelation function (ACF) to appropriate models. The simplest motion that can be addressed by this technique is random 3D diffusion of a single species, which is appropriate for small fluorescent molecules such as EGFP or Rhodamine [29]. A large protein like  $\gamma$ G, containing several spatially distinct domains, can exhibit complex diffusion behavior arising from conformational fluctuations within domains as well as relative motion of domains, necessitating the use of more complicated models for its description [30]. Here we use a model which assumes a single diffusing species (with diffusion time  $\tau_d$ ) that undergoes a chemical reaction or conformational change between two conformers, say A (fluorescent) and B (non-fluorescent), with a characteristic time constant  $\tau_r \ll \tau_d$ . The correlation function of such a system can be represented by [31]:

$$G(\tau) = \frac{1}{N} [1 + (\tau / \tau_d)]^{-1} \times [1 + (r/I)^2 (\tau / \tau_d)]^{-1/2} \bullet \left(1 + \frac{T}{1-T} e^{-\tau / \tau_r}\right) = G(\tau_d) \bullet \left(1 + \frac{T}{1-T} e^{-\tau / \tau_r}\right) \quad (1)$$

where  $T$  is the amplitude of  $\tau_r$  and represents the average fraction of molecules in the non-fluorescent (dark) state.

The result of fitting the ACF at several GdnHCl concentrations (0, 3, 5.5 and 7 M) to Eqn. (1) are shown in Fig. 4(a). Fig. 4(b) shows a superposition of the fits of an ACF (of 40 nM R- $\gamma$ G) both to Eqn. (1) and to the simple 3D diffusion model (without the contribution of conformational fluctuations, i.e.  $G(\tau_d)$ ) in the time range from 20  $\mu$ sec to 1 sec, where the effect of  $\tau_r$  (typically 7-10  $\mu$ sec) is expected to be insignificant. The fits in the overlapping region were found to be equally good, with the best fit values of  $\tau_d$  differing by 1-2% in the two cases.

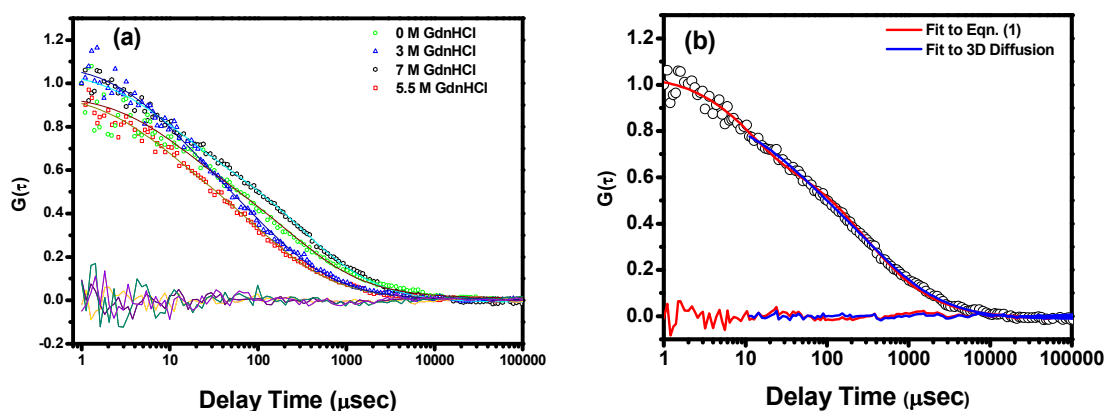


Fig. 4 a) Normalized Autocorrelation Function (ACF) of 40 nM R- $\gamma$ G in various concentrations of GdnHCl: 0 M, 3 M, 5.5M and 7M. Solid lines are fits of the data to Eq. 1 of text, while the traces at the bottom show the residuals of the fits. b) Superposition of fits of the Normalized ACF of 40 nM R- $\gamma$ G to both the conformational fluctuation model (Eqn. (1)) and a simple 3D diffusion model, together with the corresponding residuals.

FCS measurements on rhodamine B isothiocyanate-labeled  $\gamma$ G (R- $\gamma$ G) in the native state yielded a diffusion time of  $\sim 190 \mu\text{sec}$ . The hydrodynamic radius ( $R_H$ ) of a spherical diffusing species is related to diffusion time ( $\tau_D$ ) through the equation

$$\tau_D = 6\pi\eta R_H (r_0^2) / 4k_B T \quad (2)$$

where  $r_0$  is the lateral radius of the confocal volume element ( $\sim 0.204 \mu\text{m}$  in our case),  $\eta$  is the viscosity of the solution,  $k_B$  is Boltzmann's constant and  $T$  is the absolute temperature. Using this, the hydrodynamic radius of R- $\gamma$ G was calculated to be  $\sim 56 \text{ \AA}$ , agreeing well with the radius of the  $\gamma$ G molecule determined by other methods [32]. Since viscosity effects of GdnHCl were already accounted for in the normalization procedure (described in Material and Methods section),  $\eta$  was taken to be that of water for all

concentrations of GdnHCl while calculating  $R_H$ . CD spectra of Rh-labeled and unlabeled  $\gamma$ G, as well as their denaturation profiles determined by fluorescence (Fig. S1), were almost identical, confirming that labeling with Rh did not affect the structural integrity or the stability of the protein.

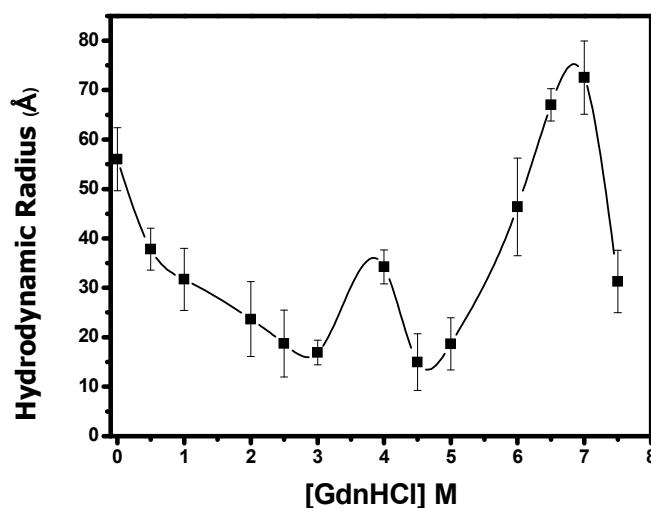


*Fig. 5 Hydrodynamic radius ( $R_H$ ) of R- $\gamma$ G in different concentrations of GdnHCl as obtained from FCS measurement.*

Fig. 5 shows a plot of the FCS-determined hydrodynamic radius ( $R_H$ ) of R- $\gamma$ G as a function of GdnHCl concentration from 0 to 7 M. If, as per conventional wisdom, the protein were to lose its structure and compactness continuously in presence of increasing denaturant concentration, there would have been a monotonous increase in  $R_H$  over the whole range studied [33]. Instead, what is observed is an unusual multi-modal dependence of  $R_H$  on the concentration of GdnHCl, a characteristic seldom found for other proteins. In particular, three key results deserve elaboration and suggest an unusual course of denaturation-induced conformational dynamics of  $\gamma$ G. First, for GdnHCl concentrations below and up to 3 M, a substantial compaction of  $\gamma$ G occurs whereby its  $R_H$  decreases from

its native-state value of 56 Å to ~20 Å. Second, on increasing the denaturant concentration further  $R_H$  exhibits a very pronounced maximum of magnitude 36 Å at 4 M GdnHCl, followed by a minimum of 15 Å at 4.5 M. Third, a further increase in [GdnHCl] from 5 M to 7 M results in a considerable expansion of the protein molecules, as evidenced by the significant increase in  $R_H$  to about 75 Å, followed by a very steep decrease of  $R_H$  to 32 Å at 7.5 M GdnHCl.

A major limitation of the conventional models used in fitting FCS data is that all of them assume a small number of diffusing species and are adequate for describing simple systems with limited heterogeneity. This approach is inadequate for extracting physically meaningful inferences from a protein solution where a large number of conformations may coexist. To overcome this problem, a model-free approach has been developed that utilizes a maximum entropy method-based algorithm (MEMFCS) to analyze the FCS data [34,35]. Using the value of  $G(\tau_d)$  Eq. (1), this analysis interprets the data in terms of a quasi-continuous distribution of particle sizes and yields the widest possible size distribution that is consistent with the data (Fig. S3a)). We have used the MEMFCS program with 150 components to analyze our FCS data. The distribution of diffusion times obtained from these fits show a single peak for all GdnHCl concentrations (Fig. S3a). It is also observed that for each GdnHCl concentration, the value of  $\tau_d$  at the peak of the distribution in Fig. S3a) agrees well with the corresponding value of  $\tau_d$  obtained by fitting the ACF to Eqn. (1) (Fig. S3b).

The decrease in  $R_H$  from 56 Å in the native state to about 20 Å at 3 M GdnHCl implies that the protein adopts a much more compact conformation in this condition. Analysis of CD spectra indicates increase in helical content and concomitant loss of random coil structure

between 0–3 M GdnHCl concentration (Fig. 3, Table S1). Since the  $F_{ab}$  and  $F_c$  domains of  $\gamma$ G are connected via random coil-rich hinge regions forming a Y-shaped structure, we propose that this compaction of  $\gamma$ G occurs through transformation of the random coil segments in the hinge region into helical structures. The helices are subsequently drawn into the hydrophobic core at the junction of the  $F_{ab}$  and  $F_c$  domains, resulting in a significant reduction of the overall spatial extent of the protein. It has been reported that proteins containing stiff lobes, such as calmodulin, undergo a preliminary compaction in hydrodynamic radius upon denaturation [36]. A study on immunoglobulin suggests that the  $F_{ab}$  and  $F_c$  fragments can retain their structural integrity when the protein is cleaved by papain digestion, which indicates the stiffness of these distinctly separated lobe-like structures [18]. Our present finding, that the native conformation of  $\gamma$ G becomes more compact upon denaturation with low concentration of GdnHCl ( $< 3$  M), is thus consistent with the reported trend.

Beyond 3 M GdnHCl  $R_H$  increases sharply, reaching a peak at 4 M. This could have been the result of aggregation of the diffusing species, but the subsequent decrease of  $R_H$  to a minimum at 5 M GdnHCl precludes that possibility as aggregation is usually an irreversible process. In any case, experimental conditions were controlled to rule out formation of aggregates. For example, the concentration of R- $\gamma$ G in all samples on which FCS measurements were carried out was 40 nM, for which the aggregation probability should be negligibly small. In addition, the reversibility of the GdnHCl-induced denaturation of R- $\gamma$ G was investigated to determine whether or not the protein molecules remained predominantly monomeric during the course of denaturation. Fig. 6 shows that the plot of the hydrodynamic radius (as calculated from the measured diffusion time) vs.

[GdnHCl] was exactly reversible within experimental errors when the unfolded protein was subjected to decreasing denaturant concentrations by serial dilution from 6.5 M GdnHCl.

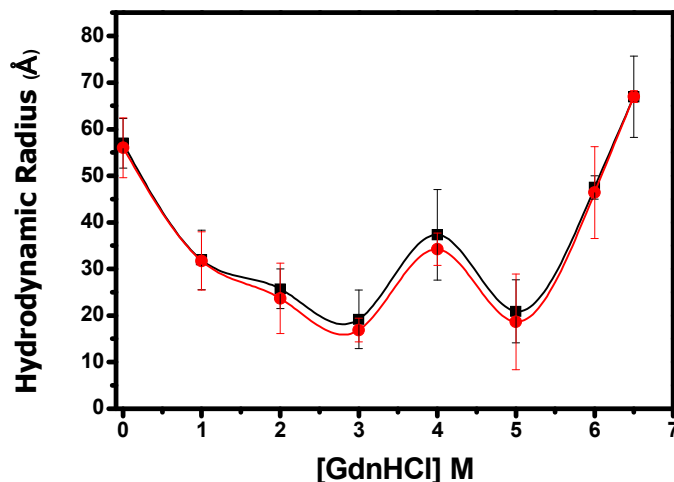


Fig. 6 Hydrodynamic radius ( $R_H$ ) of R- $\gamma$ G in different concentrations of GdnHCl during unfolding (●) and refolding (■) from 6.5 M GdnHCl.

In view of the irreversible nature of the process of aggregation, the above result established that the large values of  $R_H$  observed at 4 M and between 6 and 7 M GdnHCl could not be ascribed to diffusion of R- $\gamma$ G aggregates. This interpretation was also supported by the exact superposition of the results of fluorescence measurements of unfolding and refolding shown in Fig. 1.

In a previous FCS study on GdnHCl-induced denaturation of the F(ab')<sub>2</sub> fragment of goat anti-rabbit antibody immunoglobulin, Guo *et al.* have suggested electrostatic repulsion to be among the predominant factors leading to formation of an expanded protein ensemble at intermediate denaturant concentration (4 M GdnHCl) [33]. To test the veracity of this hypothesis we repeated the denaturation experiment in presence of 2 M NaCl in solution, both by fluorescence and FCS. Fluorescence measurements show that the trp emission maximum ( $\lambda_{max}$ ) of native R- $\gamma$ G undergoes a blue shift of 5 nm from its value in absence of

NaCl, implying that NaCl shifts the location of the trp residues into more hydrophobic regions of the protein (Fig. S2). The unfolding profile is also sharper in the transition region but the transition midpoint  $C_m$  occurs at  $(2.75 \pm 0.04)$  M GdnHCl, showing that stability is increased only marginally with NaCl addition.

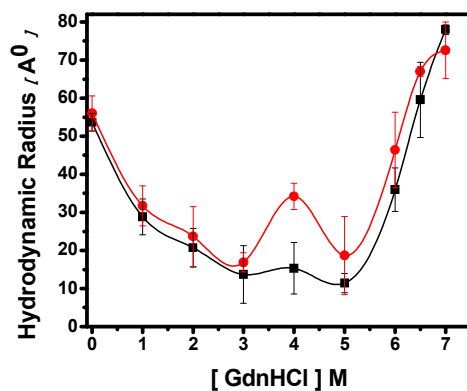


Fig. 7 Plot of hydrodynamic radius ( $R_H$ ) of  $R$ - $\gamma$ G in varying concentration of GdnHCl in presence (■) and absence (●) of 2 M NaCl.

Fig. 7 compares the results of FCS measurements in presence and absence of NaCl. Strikingly, the presence of 2 M NaCl suppressed the peak in  $R_H$  at 4 M GdnHCl – it decreases from 35 Å in absence of NaCl to 15 Å in its presence – but had little influence on the value of  $R_H$  in the range of 5-7 M GdnHCl. The result suggests that the sharp maximum of  $R_H$  between 3 and 5 M GdnHCl may actually be due to electrostatic repulsion created under denaturing condition. The expansion caused by repulsion between the charged domains of  $\gamma$ G reaches a maximum at 4 M GdnHCl before screening by guanidinium ions reverses the trend, producing a highly compact state at 5 M GdnHCl (Fig. 5).

Both GdnHCl and NaCl are salts and in solution can disrupt hydrophobic interactions and influence electrostatic forces. However  $\text{Na}^+$ , by virtue of its much smaller size ( $\sim 1\text{\AA}$ ) than  $\text{Gdn}^+$  ( $\sim 3\text{\AA}$ ), can approach the protein surface more closely and provide better electrostatic shielding than the latter, preventing formation of the expanded state at 4 M GdnHCl. Overall, these results suggest that electrostatic interactions play an important role in defining the final molecular dimensions of the denatured  $\gamma\text{G}$  molecules. Thus, while the unfolding trajectory of  $\gamma\text{G}$  is dominated by electrostatic shielding at GdnHCl concentrations up to about 4 M, electrostatic shielding by  $\text{Gdn}^+$  ions reverses the trend to bring about a compact state at higher denaturant concentrations ( $\sim 5\text{ M}$ ). Charge-charge interactions have previously been shown to play an effective role in the unfolded states of various proteins such as barstar, cytochrome c, staphylococcal nuclease and ribonuclease S [30].

The importance of electrostatic interactions was also evident in the unfolding trajectory of R- $\gamma\text{G}$  in urea (0-7 M), as measured by FCS. Urea is an uncharged denaturant which does not ionize in solution and is, therefore, not expected to cause effects similar to those ascribed to the strongly electrolytic nature of GdnHCl. Unfolding in urea produced continuous expansion of the protein (Fig. S4(a)), as evidenced by an almost monotonic increase of  $R_{\text{H}}$  with urea concentration, without the pronounced maximum observed at 4 M GdnHCl. The unfolding profile of R- $\gamma\text{G}$  determined from tryptophan emission measurement (Fig. S4(b)) showed the protein to be much more resistant to denaturation by urea than by GdnHCl, as shown by the midpoints of the transition for these two denaturants ( $C_{\text{m}} = 2.5\text{ M}$  for GdnHCl and 5.25 M for urea).

In trying to characterize the conformational dynamics of  $\gamma$ G beyond 5 M GdnHCl, it is pertinent to explore the role of disulfides in producing its drastically expanded conformational state. The disulfide bond structure of  $\gamma$ G is a consistent structural feature that is highly conserved through evolution. The two heavy chains are attached in the hinge region by disulfide bonds. Although majority of the cysteine residues are in disulfide-bonded states, free sulfhydryl groups have also been detected in  $\gamma$ G [28]. When  $\gamma$ G was preincubated with iodoacetamide to block the free sulfhydryl groups present in its native state and then denatured with increasing [GdnHCl], the increase of  $R_H$  at 7 M GdnHCl was significantly reduced (Fig. 8).

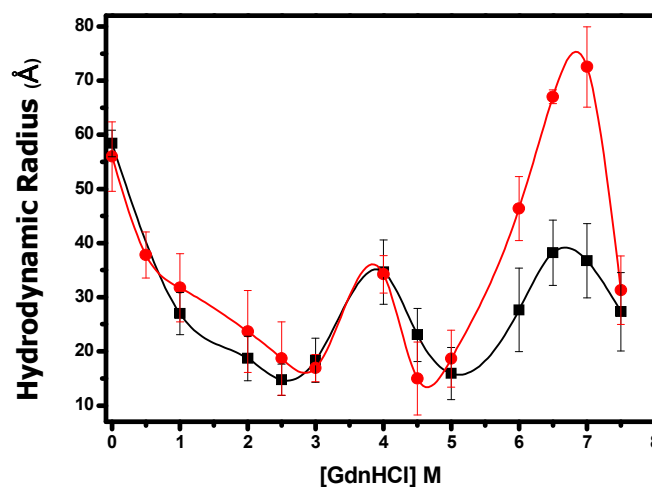


Fig. 8 Hydrodynamic radius ( $R_H$ ) of R- $\gamma$ G in varying concentration of GdnHCl in presence (■) and absence (●) of iodoacetamide.

This result points to the predominant role of free sulfhydryl groups in mediating the unusual increase in hydrodynamic radius ( $R_H \sim 72$  Å) of  $\gamma$ G when [GdnHCl] was increased further from 5 M to 7 M (in absence of iodoacetamide). Pre-incubation of  $\gamma$ G with iodoacetamide ensured that all free sulfhydryl groups present in the native protein were

modified to ensure that no rearrangement of cysteine residues to form new disulphide bonds could take place during the denaturation process leading to lower probability of structural relaxation-driven expansion of the protein, and hence to smaller  $R_H$  values (Fig. 8).

There is quite a bit of difference in the degree of solvent accessibility of inter-chain and intra-chain disulfide bonds in  $\gamma G$ . The former are well exposed to the solvent, whereas the latter are found buried deep in between two layers of anti-parallel  $\beta$ -sheet structures within each domain and are not that much solvent exposed. This difference has important consequences: the exposed cysteine residues are found to be more reactive than non-exposed ones. Though the hinge region is said to be solvent exposed, compaction caused by screening at 5 M GdnHCl leads to inaccessibility of the disulphides in the hinge region. Thus the steep rise in hydrodynamic radius beyond 5 M GdnHCl is likely due to swelling of the domains as a result of degradation of intra-chain disulphide bonds within the domains themselves, since the inter-chain disulphides in the hinge region are inaccessible under this condition. This result is consistent with the prediction of Guo *et.al.*, who earlier calculated on the basis of Flory's Scaling Law that  $R_H$  of overextended  $F_{ab}$  fragment may be as high as 113 Å.

The large and abrupt decrease in hydrodynamic radius ( $R_H$ ) from nearly 72 Å to 30 Å in presence of 7.5 M GdnHCl is very unusual and indicates substantial change in molecular weight of the diffusing species. FCS is relatively insensitive to molecular mass as can be seen from the following equation relating molecular mass to the diffusion time of globular particles (e.g. proteins):

$$\tau_D = \frac{3\pi\omega_{xy}^2\eta}{2kT} (M)^{1/3} \quad (3)$$

where  $\eta$  is the viscosity of the sample and  $M$  is the molecular mass of the fluorescent species. In practice, the diffusion times need to be sufficiently different — a factor of at least 2 — which means the molecular masses must differ by a factor of 8 [37] in order to be detected with FCS. Using Eq. 1, the apparent change in molecular weight of R- $\gamma$ G between 7 and 7.5 M GdnHCl is approximately 20 times. We have also investigated the reversibility of denaturation of  $\gamma$ G presented with 7.5 M GdnHCl. As shown in Fig. 9, renaturation from 7.5 M GdnHCl produced species with much smaller  $R_H$  ( $\sim 10$  Å), indicating that the  $\gamma$ G undergoes major conformational alteration at high GdnHCl concentration leading to formation of small molecular weight species. Fig. 9 shows that the refolding from 7.5 M GdnHCl-denatured state does not follow the same renaturation path as shown in Fig. 6, when the refolding experiments were performed from 6.5 M GdnHCl-denatured state. CD spectra indicated that the secondary structure of  $\gamma$ G was almost completely absent in 7.5 M GdnHCl (spectra were substantially noisy and not shown here). These observations led us to conclude that there is a strong possibility of fragmentation of  $\gamma$ G at very high concentration of GdnHCl (7.5 M).

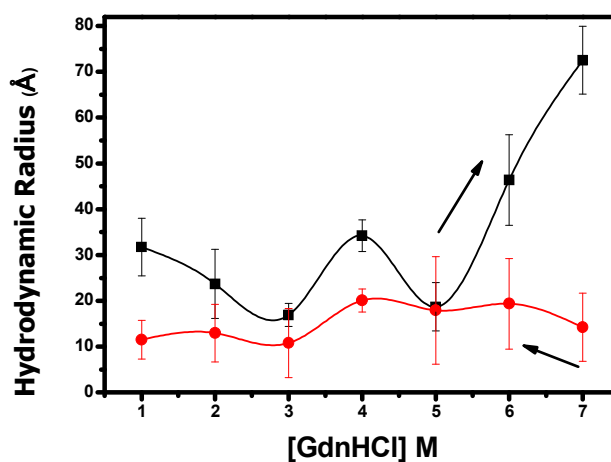


*Fig. 9 Hydrodynamic radius ( $R_H$ ) of R- $\gamma$ G during unfolding in presence of increasing concentration of GdnHCl (■) and refolding by dilution of the completely unfolded state at 7.5 M GdnHCl (●).*

### **Quantitation of free sulphydryl by DTNB assay**

A rise in concentration of free sulphydryls in  $\gamma$ G under denaturing conditions, as compared with native conditions, has been previously reported [12]. This suggests that free sulphydryl is generated from both inter- and intra-chain disulfide bonds. Because in the native conformation, inter-chain disulfide bonds have higher degree of solvent exposure, they are more prone to degradation than intra-chain disulfide bonds. Florence et al. [12, 38] has shown that under basic conditions, disulfide bonds can disintegrate through the  $\beta$ -elimination mechanism with formation of dehydroalanine and persulfide, which can further produce sulfur and cysteine. Overall, segmentation of the peptide occurs on the N-terminal side of the dehydroalanine groups and the peptide backbone is severed. Guanidine has a  $pK_a$  of  $\sim 13.6$  and at higher GdnHCl concentration  $Gdn^+$  is in equilibrium with Gdn. Thus the necessary basic condition prevails, which in turn helps in progression of the beta elimination reaction that leads to disulphide-mediated degradation. It thus appears that partial reduction of inter-chain disulfide bonds enhances the flexibility of the hinge region, resulting in detachment of the two domains.

In order to prove that GdnHCl is capable of disulphide degradation through its basic nature, we have quantified the amount of thiol produced upon denaturation using Ellman's protocol (1959) with 5,5'-dithiobis(2-nitrobenzoic acid) (Nbs<sub>2</sub>) [39]. Mixtures of  $\gamma$ G with various concentrations of GdnHCl were treated with Nbs<sub>2</sub> and their O.D. measured at 412

nm. As shown in Fig. 10 b, for a stock protein concentration of 133  $\mu\text{M}$ , the thiol produced was found to be  $\sim 75 \mu\text{M}$  in the GdnHCl aliquots 0-4 M. For  $>5 \text{ M}$  GdnHCl, a steep rise in thiol concentration (up to  $100 \mu\text{M}$ ) was observed.

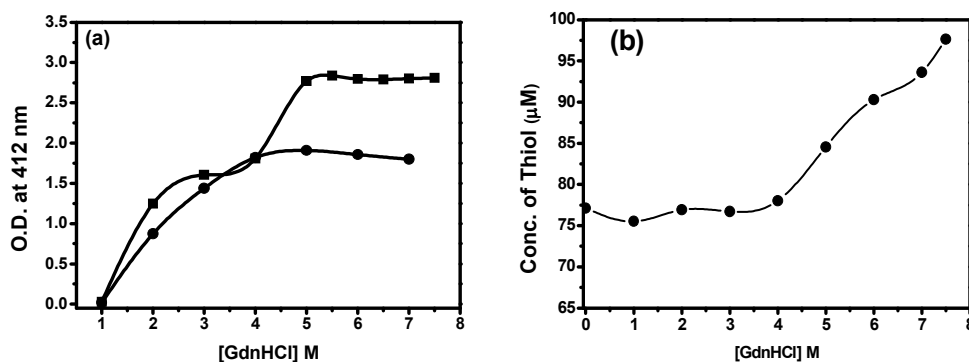


Fig. 10 (a) Dependence of O.D. (at 412 nm) of  $\text{Nbs}_2$  on GdnHCl concentration in absence (●) and presence (■) of  $\gamma\text{G}$ . The difference of O.D. between the two curves is proportional to the amount of free thiol produced by degradation of disulphides in  $\gamma\text{G}$ . (b) Plot of thiol concentration versus GdnHCl concentration.

It is clear that thiol production is on average constant for GdnHCl concentrations below 5 M, implying that GdnHCl at lower concentrations (0-4 M) does not contribute to disulphide degradation. However, thiol concentration increases at higher concentration of GdnHCl (5 M onwards) and reaches a saturation concentration of  $\sim 100 \mu\text{M}$  at  $\sim 7 \text{ M}$  GdnHCl, indicating that GdnHCl is effective in disulphide degradation. This result is in agreement with our hypothesis that the initial rise in  $R_{\text{H}}$  after 5 M GdnHCl is due to intra-chain disulfide bond degradation and thereafter loss of molecular weight of  $\gamma\text{G}$  occurs due to fragmentation at the hinge region via disulphide degradation.

## Conclusions

In a nutshell, the observations described above lead us to propose a scheme for the intricate dynamics of conformational transitions of the multi-domain protein  $\gamma$ G. It is proposed that low concentrations of GdnHCl (up to 3 M) induce helix formation in the hinge region, which results in marked compaction of  $\gamma$ G (56 Å to 20 Å). But interestingly, 4 M GdnHCl causes significant swelling of  $\gamma$ G, most likely due to electrostatic repulsion. Higher concentration of Gdn<sup>+</sup> and Cl<sup>-</sup> (5 M) can give rise to a shielding effect that reduces the electrostatic repulsion and again leads to a compact conformation. Even more increase in GdnHCl concentration disrupts the protein structure significantly leading to loosening of compact globular domains held together by mostly non-covalent and disulphide bonds. We speculate that the huge expansion in the hydrodynamic radius of  $\gamma$ G in presence of 7 M GdnHCl was due to formation of unordered and expanded conformations, aided by degradation of intra-chain disulphide bonds. The decrease in  $R_H$  at 7.5 M GdnHCl and DTNB assay signals degradation of inter-chain disulphide bonds via beta elimination reaction, resulting in fragmentation of  $\gamma$ G to smaller molecular weight species.

## Materials and Methods

All reagents, including bovine Gamma globulin, iodoacetamide, GdnHCl (8 M solution), sodium di-hydrogen phosphate, di-sodium hydrogen phosphate, rhodamine B isothiocyanate and dimethyl sulfoxide (DMSO) were purchased from Sigma-Aldrich (USA) and were of highest available purity. Triple distilled water from MilliQ source, Millipore Corporation (USA) was used for preparation of phosphate buffer. Denaturation experiments were carried out in 10 mM phosphate buffer, pH 7.4. The working

concentration of  $\gamma$ G was 40 nM for FCS measurements and 1  $\mu$ M for fluorescence and CD spectroscopy.

### ***Fluorescent labeling of $\gamma$ G***

The protein (8 mg/ml) was dissolved in 10 mM phosphate buffer, pH 7.4, at room temperature. A solution of 0.3 mg Rhodamine B isothiocyanate (RhB) in 500  $\mu$ l DMSO was slowly added to this solution with constant stirring in nitrogen environment. The molar ratio of the dye and the protein was kept at 10:1. The resulting solution was incubated with shaking for 3 hrs at 4°C and then dialyzed extensively against 10 mM phosphate buffer, pH 7.4 with change of buffer after every 6 hours to remove the free RhB. Further free RhB was removed by passing the dialyzed solution through a Sephadex G20 column equilibrated with 20 mM sodium phosphate buffer (pH 7.4) [20]. The rhodamine labeled protein thus obtained is denoted as R-  $\gamma$ G.

### ***Spectroscopic Measurements***

A Jasco V-650 absorption spectrophotometer (Jasco, Japan) and Hitachi F-7000 spectrofluorometer were used for absorption and emission spectral studies, respectively, using a quartz cuvette of path length 1 cm. Excitation and emission bandwidths were kept at 2.5 nm for all fluorescence measurements. Denaturation was carried out by preparing a set of aliquots of 1  $\mu$ M  $\gamma$ G in GdnHCl solutions of varying concentration (0.5 M to 7.5 M) and leaving them aside for at least one hour to ensure maximum denaturing action of GdnHCl. Trp fluorescence emission spectra, with excitation at 295 nm, were recorded for each of the aliquots and the wavelengths at emission maxima ( $\lambda_{\text{max}}$ ) evaluated.

Renaturation experiments were performed by serial dilution of the aliquot, containing  $\gamma$ G denatured with 6.5 M GdnHCl, with phosphate buffer to arrive at gradually decreasing

concentrations of GdnHCl (6.5 to 1 M) and measuring the wavelength at fluorescence emission peak under the modified conditions. The sample corresponding to 0 M GdnHCl was obtained by dialyzing out GdnHCl from the sample having 1 M GdnHCl.

Denaturation experiments were also performed using CD spectroscopy. CD spectra of  $\gamma$ G in various GdnHCl concentrations were collected on a Chirascan CD spectrometer (Applied Photophysics, UK) using a rectangular cuvette of path length 0.1 mm and averaging five successive scans between 190 and 260 nm at a scan speed of 20 nm/min. The secondary structure content of the protein at a particular concentration of GdnHCl was calculated by analyzing its CD spectrum using the online fitting program CDSSTR (available free of charge on the website <http://dichroweb.cryst.bbk.ac.uk>), which allows estimation of relative contents of the four main types of secondary structures, viz. helix, sheet, turn and random coil, from the CD spectrum of a protein [24-26].

### ***Fluorescence Correlation Spectroscopy (FCS)***

FCS probes the fluctuations in fluorescence intensity induced by alterations in the excited singlet or triplet-state population, variation in concentration due to translational motion of the fluorophores in and out of the confocal volume, or changes in their physicochemical properties due to a chemical reaction or due to complexation. The normalized autocorrelation function  $G(\tau)$  of the intensity fluctuations  $\delta F(t)$ ,

$$\delta F(t) = F(t) - \langle F \rangle \quad (4)$$

indicates the variation in the probability to register a second photon from the same molecule at the correlation time  $\tau$ , once a first was emitted:

$$G(\tau) = \frac{\langle \delta F(t+\tau) \delta F(t) \rangle}{\langle F(t) \rangle^2} \quad (5)$$

If the fluorescence intensity fluctuations arise only from translational diffusion, the time-dependent part of the correlation function is given by:

$$G(\tau) = \frac{1}{\langle N \rangle} [1 + (\tau / \tau_d)]^{-1} \times [1 + (r/l)^2 (\tau / \tau_d)]^{-1/2} \quad (6)$$

or, 
$$G(\tau) = \frac{1}{\langle N \rangle} f\left(\frac{\tau}{\tau_d}\right)$$
 with

$$f\left(\frac{\tau}{\tau_d}\right) = [1 + (\tau / \tau_d)]^{-1} \times [1 + (r/l)^2 (\tau / \tau_d)]^{-1/2}$$

where  $l$  and  $r$  are the half axes of the excitation volume perpendicular along and to the laser beam,  $\langle N \rangle$  is the mean number of fluorophores within the confocal volume and  $\tau_d$  is the translational diffusion time of the molecules across the sample volume. The translational diffusion coefficient  $D$  is related to  $\tau_d$  by:

$$r^2 = 4D\tau_d \quad (7)$$

The value of  $G(\tau)$  at  $\tau = 0$  gives the inverse of the number of fluorescent molecules in the observation volume, i.e.  $G(0) = 1/N$ .

During the FCS measurements, five successive time series of fluorescence intensity data (each of duration 30 sec) were collected on each sample of R- $\gamma$ G at a given GdnHCl concentration. Each time series was processed to extract the intensity autocorrelation function (ACF), which was then fitted to an appropriate diffusion model (Eq. 1 above) to extract the diffusion time ( $\tau_d$ ). The  $\tau_d$  values so obtained are influenced by change in apparent size of the focal volume due to mismatch in the index of refraction between the solution and the sample holder, as well as significant change in viscosity of GdnHCl solution. To account for both these effects, the change in  $\tau_d$  of free RhB (40 nM) was measured as a function of GdnHCl concentration and the  $\tau_d$  value for the protein at a

particular GdnHCl concentration  $c$  was normalized by a multiplicative factor equal to the ratio  $(\tau_d)_0/(\tau_d)_c$  for RhB, where the subscript 0 refers to aqueous solution. (19, 20, 40-42)

Error bars of  $R_H$  shown in Figs. 5-9 were calculated from the standard error of the mean of each  $\tau_d$  from its five determinations for each sample.

### Acknowledgement

We sincerely thank Prof. Sudipta Maiti of TIFR, Mumbai for assistance in setting up the FCS apparatus at Saha Institute. We acknowledge financial support from CSIR, Govt. of India and the BARD Project at Saha Institute.

### References

1. Royer, C. A. 2006. Probing Protein Folding and Conformational Transitions with Fluorescence. *Chem. Rev.* 106: 1769-1784.
2. Dill, K. A. 1991. Denatured states of proteins. *Annu. Rev. Biochem.* 60:795-825.
3. Haustein, E., and P. Schwille. 2007. Fluorescence Correlation Spectroscopy: Novel Variations of an Established Technique; *Annu. Rev. Biophys. Biomol. Struct.* 36:151-169.
4. Vukojevic, V., A. Pramanik, T. Yakovleva, R. Rigler, L. Terenius and G. Bakalkina. 2005. Study of molecular events in cells by fluorescence correlation spectroscopy. *Cell. Mol. Life Sci.* 62: 535–550.
5. Sikor, M., and I.O.B. Weillheim. 2011. Single-molecule fluorescence studies of Protein Folding and Molecular Chaperones.
6. Fitter J. 2009. The perspectives of studying multi-domain protein folding. *Cell. Mol. Life Sci.* 66:1672-81.

7. Batey S., Nickson A. A., Clarke J. 2008. Studying the folding of Multidomain proteins. *HFSP Journal*. 2: 365–377.
8. Kindt T. J., B. A. Osborne, R. A. Goldsby. 2006. *Kuby Immunology*, 6th Edition, W.H. Freeman Publishers: Biology.
9. Bork, P., L. Holm, C. Sander. 1994. The immunoglobulin fold - structural classification, sequence patterns and common core. *J Mol Biol*. 242:309–320.
10. Lilie, H., J. Buchner. 1995. Domain interactions stabilize the alternatively folded state of an antibody  $F_{ab}$  fragment. *FEBS Letters*. 362:43–46.
11. Rothlisberger, D., A. Honegger, A. Pluckthun. 2005. Domain interactions in the  $F_{ab}$  fragment: A comparative evaluation of the single-chain  $F_c$  and  $F_{ab}$  format engineered with variable domains of different stability. *J Mol Biol*. 347:773–789.
12. Liu, H., and K. May. 2012. Disulfide bond structures of IgG molecules Structural variations, chemical modifications and possible impacts to stability and biological function; *mAbs*. Landes Bioscience. 4:17-23.
13. Lilie, H. 1997. Folding of the  $F_{ab}$  fragment within the intact antibody. *FEBS Letters*. 417:239–242.
14. Goto, Y., K. Hamaguchi. 1982. Unfolding and refolding of the constant fragment of the immunoglobulin light chain. *J Mol Biol*. 156:891–910.
15. Goto, Y., K. Hamaguchi. 1982. Unfolding and refolding of the constant fragment of the immunoglobulin light chain - kinetic role of the intrachain disulfide bond. *J Mol Biol*. 156:911–926.

16. Lilie, H., R. Rudolph, J. Buchner. 1995. Association of antibody chains at different stages of folding: prolyl isomerization occurs after formation of quaternary structure. *J Mol Biol.* 248:190–201.
17. Feige, M.J., F. Hagn, J. Esser, H. Kessler, J. 2007. Buchner Influence of the internal disulfide bridge on the folding pathway of the C-L antibody domain. *J Mol Biol.* 365:1232–1244.
18. Arnoldus, W., P. Vermeer, W. Norde, A.V. Amerongen. 2000. The Unfolding/Denaturation of Immunoglobulin of Isotype 2b and its F<sub>ab</sub> and F<sub>c</sub> Fragments. *Biophys J.* 79: 2150-4.
19. Frieden, C., K. Chattopadhyay, E.L. Elson. 2002. What fluorescence correlation spectroscopy can tell us about unfolded proteins. *Adv. Protein Chem.* 62:91–110.
20. Chattopadhyay, K., S. Saffarian, E. L. Elson, C. Frieden. 2005. Measuring unfolding of proteins in the presence of denaturant using fluorescence correlation spectroscopy. *Biophys J.* 88:1413–1422.
21. Magde, D., E.L. Elson, W.W. Webb. 1974. Fluorescence correlation spectroscopy II. Experimental realization *Biopolymers.* 13:29–61.
22. Corrêa, D. H. A., C. H. I. Ramos. 2009. The use of circular dichroism spectroscopy to study protein folding form and function. *Afr. J. Biochem. Res.* 3:164-173.
23. Khan, F., A. Ahmad and M. I. Khan. 2007. Chemical, Thermal and pH-induced Equilibrium Unfolding Studies of *Fusarium solani* Lectin. *IUBMB Life*, 59: 34 – 43.
24. Whitmore, L. and B.A. Wallace. 2008. Protein Secondary Structure Analyses from Circular Dichroism Spectroscopy: Methods and Reference Databases. *Biopolymers.* 89:392-400.

25. Whitmore, L. and B.A. Wallace. 2004. DICHROWEB: an online server for protein secondary structure analyses from circular dichroism spectroscopic data. *Nucleic Acids Res.* 32:W668-673.
26. Lobley, A., L. Whitmore, and B.A. Wallace. 2002. DICHROWEB: an interactive website for the analysis of protein secondary structure from circular dichroism spectra. *Bioinformatics* 18:211-212.
27. Hall, V., M. Sklepari and A. Rodger. 2014. Chirality Protein Secondary Structure Prediction from Circular Dichroism Spectra Using a Self-Organizing Map with Concentration Correction. 26:471–482.
28. Vlasak J., R. Ionescu. 2011. Fragmentation of monoclonal antibodies. *Landes Bioscience* 3:253-263.
29. Jeyasekharan A. D., N. Ayoub, R. Mahen, J. Ries, A. Esposito, E. Rajendra, H. Hattori, R. P. Kulkarni, A. R. Venkitaraman. 2010. DNA damage regulates the mobility of Brca2 within the nucleoplasm of living cells. *Proc. Nat. Acad. Sc.* 107:21937–21942.
30. Schwille P., U. Haupts, S. Maiti, W. W. Webb. 1999. Molecular Dynamics in Living Cells Observed by Fluorescence Correlation Spectroscopy with One- and Two-Photon Excitation. *Biophys. J.* 77:2251–2265.
31. Haupts, U., S. Maiti, P. Schwille, and W.W. Web. 1998. Dynamics of fluorescence fluctuations in green fluorescent protein observed by fluorescence correlation spectroscopy, *Proc. Natl. Acad. Sci. U.S.A.* 95:13573-13578.
32. Patel H. M., J. L. Kraszewski, B. Mukhopadhyay. 2004. *J. Bacteriol.* 186:5129–5137
33. Guo, L., P. Chowdhury, J. M. Glasscock, and F. Gai. 2008. Denaturant induced expansion and compaction of a multi-domain protein: IgG. *J. Mol. Biol.* 384: 1029–1036.

34. Garai, K., P. Sengupta, B. Sahoo and S. Maiti. 2006. Selective destabilization of soluble amyloid beta oligomers by divalent metal ions. *Biochem Biophys Res Commun.* 23:210–215.
35. Nag, S., B. Sarkar, A. Bandyopadhyay, B. Sahoo, V.K.A. Sreenivasan, M.K.C. Muralidharan and S. Maiti. 2011. Nature of the amyloid- $\beta$  monomer and the monomer-oligomer equilibrium. *J Biol. Chem.* 286:13827–13833.
36. Haustein, E. and P. Schwille. 2003. Ultrasensitive investigations of biological systems by fluorescence correlation spectroscopy. *Methods* 29:153–166.
37. Schwille P., E. Haustein. 2004. *Fluorescence Correlation Spectroscopy: An Introduction to its Concepts and Applications.* Biophys. J. 1-32.
38. Florence, T. M., 1980. Degradation of protein disulphide bonds in dilute alkali *Biochem. J.* 189:507-520.
39. Ellman, G. L., 1959. Tissue sulfhydryl groups. *Arch. Biochem. Biophys.* 82:70-77.
40. Starr, T.E., N.L. Thompson. 2002. Local diffusion and concentration of IgG near planar membranes: Measurement by total internal reflection with fluorescence correlation spectroscopy. *J. Phys. Chem B.* 106:2365–2371.
41. Nag M., K. Bera, S. Chakraborty, S. Basak. 2013. Sensing of hydrophobic cavity of serum albumin by an adenosine analogue: Fluorescence correlation and ensemble spectroscopic studies. *J. Photochem. Photobiol. B.* 127: 202–211.
42. Nag M., K. Bera, S. Basak. 2015. Intermolecular disulfide bond formation promotes immunoglobulin aggregation: Investigation by fluorescence correlation spectroscopy. *Proteins: Structure, Function, and Bioinformatics.* 83:169–177.